Inorganic Chemistry

Article

pubs.acs.org/IC

# CopC Protein from *Pseudomonas fluorescens* SBW25 Features a Conserved Novel High-Affinity Cu(II) Binding Site

Chathuri J. K. Wijekoon, Tessa R. Young, Anthony G. Wedd, and Zhiguang Xiao*

School of Chemistry and Bio21 Molecular Science and Biotechnology Institute, University of Melbourne, Parkville, Victoria 3010, Australia

Supporting Information

**ABSTRACT:** Copper homeostasis in the bacterium *Pseudomonas fluorescens* SBW25 appears to be mediated mainly via chromosomal *cue* and *cop* systems. Under elevated copper levels that induce stress, the *cue* system is activated for expression of a $P_{1B}$-type ATPase to remove excess copper from the cytosol. Under copper-limiting conditions, the *cop* system is activated to express two copper uptake proteins, *Pf*-CopCD, to import this essential nutrient. *Pf*-CopC is a periplasmic copper chaperone that may donate copper to the inner membrane transporter *Pf*-CopD for active copper importation. A database search revealed that *Pf*-CopC belongs to a new family of CopC proteins (designated Type B in this work) that differs significantly from the known CopC proteins of Type A that possess two separated binding sites specific for Cu(I) and Cu(II). This article reports the isolation and characterization of *Pf*-CopC and demonstrates that it lacks a Cu(I) binding site and possesses a novel Cu(II) site that binds Cu(II) with 100 times stronger affinity than do the Type A proteins. Presumably, this is a requirement for a copper uptake role under copper-limiting conditions. The Cu(II) site incorporates a highly conserved amino terminal copper and nickel (ATCUN) binding motif, $NH_2$-Xxx-Xxx-His, but the anticipated ATCUN binding mode is prevented by a thermodynamically more favorable binding mode comprising His1 as a key bidentate ligand and His3 and His85 as co-ligands. However, upon His1 mutation, the ATCUN binding mode is adopted. This work demonstrates how a copper chaperone may fine tune its copper binding site to meet new challenges to its function.

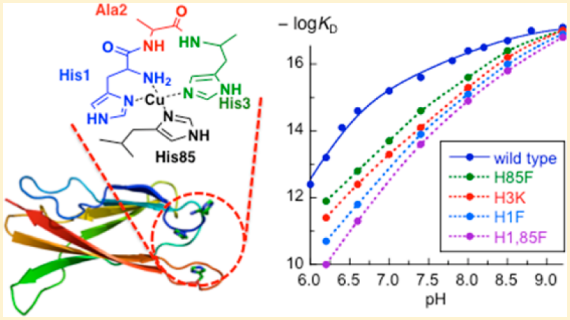


## INTRODUCTION

Copper is a redox-active metal whose relevant oxidation states, Cu(I) and Cu(II), exhibit high affinities for almost all metal sites in biomolecules. Such properties have led to its evolution as an essential cofactor in the catalytic sites of a wide range of enzymes, including cytochrome c oxidase for respiration, superoxide dismutase for antioxidant defense, ceruloplasmin for iron uptake, and monooxygenases and multicopper oxidases for substrate oxidation (including detoxification of Cu(I)).[1−3] However, when not under proper control, these same properties have the potential to cause damage to cells. Undesirable redox chemistry may lead to catalytic generation of reactive oxygen species (ROS) and other toxic products, and the dominant affinities may result in displacement of other essential metals from their native sites. Consequently, a delicate balance must be maintained between deficiency and excess, and specific homeostatic mechanisms have evolved to control copper metabolism.[1−6]

Several copper regulation systems have been identified and characterized in Gram-negative bacteria, including the *cue*, *cus*, and *cop*/*pco* operons.[1−3,7] The *cue* system encodes a transmembrane $P_{1B}$-type ATPase and, in many cases, also a multicopper oxidase such as CueO in *Escherichia coli*. The former is a central component for Cu(I) efflux across the cell membrane, and the latter is a periplasmic cuprous oxidase that is able to oxidize certain stable Cu(I) complexes to less toxic Cu(II) forms under aerobic conditions.[8−10] It is believed that one role of CueO is to support the Cu(I) efflux function of the ATPase for copper tolerance.[11]

The *cus* system in *E. coli* contains four proteins, CusABCF.[12] CusA is an inner membrane copper pump that is connected to the outer membrane pore CusC via the linker CusB to form a tripartite complex CusCBA that spans the periplasmic space.[13−15] It is capable of removing excess Cu(I)/Ag(I) directly from the cytosol. The fourth Cus member, CusF, is a periplasmic copper chaperone that appears to expel excess Cu(I)/Ag(I) from the periplasm via the CusCBA complex.[16] The *cus* system plays an important role in copper tolerance under anaerobic conditions when the *cue* system is not functioning.[17]

Some bacteria have evolved copper resistance based upon additional plasmid-borne *cop*/*pco* operons. The *pco* operons in *E. coli* comprise seven genes, *pcoABCDpcoRSpcoE*, and expression of proteins PcoABCDE is regulated by the two-component system, PcoRS.[18] Three soluble proteins (PcoA, PcoC, PcoE) are expressed to the periplasm, and two copper permeases (PcoB, PcoD) are present in the outer and inner

**Received:** January 5, 2015
**Published:** February 24, 2015





DOI: 10.1021/acs.inorgchem.5b00031
*Inorg. Chem.* 2015, 54, 2950−2959

membranes, respectively. PcoA is a multicopper oxidase with cuprous oxidase activity.[19,20] PcoC is a copper chaperone with two separated binding sites specific for Cu(I) and Cu(II).[21] When loaded with both copper ions (i.e., as $Cu^{I}Cu^{II}$–PcoC), the protein is air-stable. PcoA is able to catalyze aerial oxidation of the Cu(I) ion bound in $Cu^{I}Cu^{II}$–PcoC and to release it as less toxic $Cu_{aq}^{2+}$.[20] PcoE is specific for the *pco* system. It appears to be a sponge for monovalent metal ions such as Cu(I)/Ag(I)[22] and was postulated to initially sequester Cu in the periplasm before the other *pco* genes are fully induced.[23] The *cop* operons found in the copper resistance bacterium *Pseudomonas syringae* carry six genes, *copABCDcopRS*, with equivalent functions and protein products as those of their *pco* counterparts, suggesting a conserved mechanism of copper resistance.[21,24]

Genes homologous to the plasmid-borne *cop*/*pco* system are also present in the chromosomes of many bacteria, including *E. coli* and *P. syringae*. In contrast, the plant growth-promoting bacterium *Pseudomonas fluorescens* SBW25 features a chromosomal *cop* operon encoding two Cop proteins, CopCD, only, rather than the usual four proteins, CopABCD.[25] Expression of the *copCD* genes is controlled by copper levels and mediated by a CopRS regulatory system. Mutants devoid of *copCD* or *copS* are more tolerant to copper, whereas overexpression of CopCD increases copper sensitivity. This behavior suggests that *Pf*-CopCD may have evolved to import the essential metal under copper-limiting conditions.[25] Like other Gram-negative bacteria, *P. fluorescens* SBW25 also carries a *cue* system that, in response to elevated copper levels, activates expression of an efflux pump, CueA (another $P_{1B}$-type ATPase), under the control of a MerR-like regulator CueR. Thus, the *cop* and *cue* systems in this case are integral to copper homeostasis, with the *cop* operon being activated at low copper levels to import nutrient copper into the cell and the *cue* operon being activated under copper stress to expel excess metal ion from the cell.

Interestingly, an earlier study showed that copper-resistant *P. syringae* cells carrying the resistance operon *copABCD* become hypersensitive to copper when *copCD* devoid of *copAB* was expressed.[26] This observation was also consistent with a copper uptake role for proteins *Ps*-CopCD. A similar uptake role has been assumed for the *E. coli* homologue, *Ec*-PcoCD.[22] It was suggested that this function may be required to compensate for the copper-sequestering activity of other Cop/Pco proteins to ensure an adequate supply of nutrient copper.[27] However, operons *Pf-copCD* and *Ps-copABCD*/*Ec-PcoABCD* operate at low and high copper concentrations, respectively. Protein *Pf*-CopD is similar to *Ps*-CopD/*Ec*-PcoD. They are all inner membrane proteins with a predicted structure featuring eight transmembrane domains that are rich in the Cu(I) ligands Met and Cys and are expected to transport Cu(I). *Pf*-CopC is also similar to *Ps*-CopC/*Ec*-PcoC in overall protein sequence; however, *Pf*-CopC lacks the side chains anticipated for a Cu(I) site and has an altered sequence for the expected Cu(II) site. Consequently, the copper binding chemistry of *Pf*-CopC is expected to be different from that of *Ps*-CopC/*Ec*-PcoC.

A database search identified a large family of proteins similar to *Pf*-CopC, but none has been isolated for in vitro characterization. The family is designated Type B to distinguish it from the known Type A that binds Cu(I) and Cu(II) at separated high-affinity sites. This work has expressed and isolated *Pf*-CopC and demonstrated that, while it has a low affinity for Cu(I), it carries a novel Cu(II) site with subfemtomolar affinity at pH 7.4. This affinity is about 2 orders of magnitude higher than the affinities of Type A proteins. Such high affinity may be needed for a copper chaperone role under copper-limiting conditions.

## EXPERIMENTAL SECTION

**Materials and General Procedures.** Cu(I) ligands bicinchoninic anion (Bca) and bathocupröine disulfonate (Bcs), Cu(II) ligands glycine (Gly), histidine (His), *N,N,N′,N′*-ethylenediaminetetraacetic acid (Edta), and *N*-(2-hydroxyethyl)ethylenediamine-*N,N′,N′*-triacetate (HEdta) and pH buffers *N*-cyclohexyl-2-aminoethanesulfonic acid (Ches), 4-(2-hydroxyethyl)-1-piperazineethanesulfonic acid (Hepes), 2-(*N*-morpholino)ethanesulfonic acid (Mes), 3-(*N*-morpholino)-propanesulfonic acid (Mops), and tris(hydroxymethyl)aminoethane (Tris) were all purchased from common commercial sources without further purification. Cu(II) probes DP2 (dansyl peptide 2 (DAE-($K^{DNS}$)RHDH)), DP3 (dansyl peptide 3 (HP($K^{DNS}$)DHDH)), and DP4 (dansyl peptide 4 (H($K^{DNS}$)HH)) were synthesized as reported.[28] The concentration of each DP probe was determined by the solution absorbance at 326 nm using a reported $\varepsilon$ = 4500 $M^{-1}$ $cm^{-1}$ for all DP probes.[28] The concentration of HEdta was calibrated via titration of a standard solution of Cu(II) into a mixture containing HEdta and probe DP2, as described recently.[28] The Cu(II) standard was prepared by dissolving $CuSO_4 \cdot 5H_2O$ in Milli-Q water and calibrated via reaction with excess Cu(I) ligand Bcs in Mops buffer containing reductant $NH_2OH$. Under such conditions, all copper ions were converted quantitatively to the well-defined chromophoric complex anion $[Cu^{I}(Bcs)_2]^{3-}$ with intense absorbance at 483 nm ($\varepsilon$ = 13 000 $M^{-1}$ $cm^{-1}$).[29]

**Bioinformatics Analysis and Structural Modeling.** Protein homologues of *Pf*-CopC and *Ec*-PcoC in the NCBI database were searched via BLAST using the relevant protein sequence as the query sequence. The returned sequence homologues were selected and aligned using program ClustalW.[30] The structural modeling of *Pf*-CopC was performed with SWISS-MODEL software using the NMR structure of *Ps*-CopC (PDB code: 1NM4) as a template.[31]

**Construction of Expression Plasmids and Site-Directed Mutagenesis.** The *Pf*-CopC gene coding the whole protein sequence including the signal peptide (GenBank access no. YP_002873498) was synthesized by Bio Basic Inc. (Canada) with the expression condons optimized for expression in *E. coli*. The gene was cloned into expression vector pET20b between restriction sites NdeI and BamHI to construct a *Pf*-CopC expression plasmid. Site-directed mutagenesis was performed by PCR using the wild-type (wt) CopC gene as a template to generate the equivalent plasmids for expression of protein variants *Pf*-CopC-H1F, -H3K, -H85F, and -H1,85F.

**Protein Expression and Purification.** Each expression plasmid was propagated with *E. coli* Top10 and transformed into BL21(DE3) CodonPlus cells for protein expression. The transformed cells were grown in 2YT medium containing ampicillin (100 mg/L) and chloramphenicol (34 mg/L) in shaking flasks at 37 °C to $OD_{600}$ ~ 1, followed by induction of protein expression overnight at ~30 °C with IPTG at a final concentration of 0.5 mM. The cells were harvested by centrifugation.

A clarified cell extract was prepared in Tris-Cl buffer (10 mM; pH 8.0), and the subsequent protein purification procedures varied for different forms of the CopC proteins. For proteins *Pf*-CopC and its H3K variant, the cell extract was adjusted to pH 6.0 with a minimal volume of Mes solution (~200 mM) and then applied to a CM-52 cation-exchange column. The bound CopC proteins were eluted with a salt gradient of NaCl (0–500 mM) in Mes buffer (20 mM, pH 6.0). For H1F and H85F variants of weaker affinity for the CM-52 column, the cell extract solution was adjusted to pH ~ 5.0 with acetic acid and then purified with an SP Sepharose fast flow cation-exchange column in acetate buffer (20 mM, pH 5.0). The H1,85F protein did not bind efficiently to cation-exchange columns but was retained on a source-Q anion-exchange column at pH 8.5. The first step of its purification employed a NaCl gradient elution from the Source-Q column in Tris buffer at pH 8.5. Edta (1.0 mM) was included in the elution buffer of the first-step purification in each case to ensure removal of any


DOI: 10.1021/acs.inorgchem.5b00031
*Inorg. Chem.* 2015, 54, 2950–2959

contaminating metal ions. The ion-exchange fractions containing the target proteins were concentrated, applied to a Superdex 75 gel-filtration column (HR16/60; GE Healthcare), and eluted with Mops buffer (20 mM, pH 7.4; NaCl, 100 mM). Purity and identity of each isolated protein were confirmed by SDS-PAGE and ESI-MS (see Table S1). Protein yields were in the range 15−25 mg per 1 L of culture.

Proteins CopC from *P. syringae* (*Ps*-CopC) and PcoC from *E. coli* (*Ec*-PcoC) were expressed and isolated as reported previously.[21,24] Their concentrations were estimated from their solution spectra using reported molar absorptivities $\varepsilon(280)$ of 8700 and 10 100 $M^{-1}$ $cm^{-1}$, respectively.[21,24] The protein concentrations for all *Pf*-CopC proteins were estimated using $\varepsilon(280)$ = 8480 $M^{-1}$ $cm^{-1}$, calculated from their amino acid compositions. These estimates were verified by fluorescence titration of each protein with a $Cu^{2+}$ standard (cf. Figure S1).

**Spectroscopic Approaches.** UV−visible spectra were recorded on a Varian Cary 300 spectrophotometer in dual-beam mode with quartz cuvettes of 1.0 cm path length. All metal titrations were performed in appropriate buffers and corrected for baseline and dilution. Far UV CD spectra were recorded on a Chirascan-plus spectrometer (Applied Photophysics) using a 0.1 cm quartz cell. Three scans were averaged, and a baseline was subtracted from each recorded spectrum. Fluorescence emission spectra were recorded on a Varian Cary Eclipse spectrophotometer with a band-pass of 20 nm for both excitation and emission. The excitation wavelength for the dansyl peptide (DP) probes was 330 nm, and the emission spectra were recorded between 450 and 750 nm at a scan rate of 600 nm $min^{-1}$. The excitation wavelength for other peptides or proteins was 280 nm with a recorded spectral range between 295 and 500 nm. Electron paramagnetic resonance (EPR) spectra were recorded on Bruker Elexsys E 500 EPR spectrometer with the following instrument conditions: microwave frequency, 9.456−9.495 GHz; microwave power, ∼1 mW; modulation amplitude, 4 G; sweep time, 100 s; time constant, 50 ms; and average number of scans, 10. All Cu(II)−protein samples were purified from either an anion or cation ion-exchange column as a single component and were prepared at 0.5 mM concentration in Mops buffer (100 mM, pH 7.4) containing ∼10% glycerol. The samples were snap-frozen in liquid nitrogen, and the spectra were recorded at 77 K in a liquid-nitrogen finger Dewar. The EPR parameters ($g$ values and $A$ values) were extracted directly from the recorded spectra without simulation.

**Quantification of Cu(II) Binding Stoichiometry via Direct Metal Ion Titration.** *Pf*-CopC protein and its four protein variants emit intense fluorescence at $\lambda_{max}$ ∼ 335 nm upon excitation at $\lambda_{ex}$ ∼ 280 nm, attributable to the presence of Trp77 in the protein sequences. Cu(II) binding quenches the fluorescence intensity linearly until the binding site(s) are saturated. The binding stoichiometry was determined in each case by direct titration of each protein solution (5.0 $\mu$M, 2.0 mL) in an appropriate buffer with a $CuSO_4$ standard (200 $\mu$M).

**Quantification of Cu(II) Binding Affinity via Ligand Competition.** The Cu(II) binding affinities expressed as dissociation constants ($K_D$) were determined via ligand competition using two Cu(II)-responsive fluorescence probes, DP3 and DP4, that were described recently.[28] These probes are short peptides containing a dansyl fluorophore attached to the side-chain of a lysine residue and bind Cu(II) with log $K_D$ = −12.3 for DP3 and −14.1 for DP4 at pH 7.4. They emit intense fluorescence at $\lambda_{max}$ ∼ 550 nm upon excitation at ∼330 nm, and binding of Cu(II) quenches the fluorescence intensity. The determination was based on eqs 1−4 for the competition for Cu(II) between the DP probe (P) and the protein target (T).[28]

$$Cu^{II}P + T \rightleftharpoons Cu^{II}T + P \quad (1)$$

$$K_{ex} = \frac{[Cu^{II}T][P]}{[Cu^{II}P][T]} = \frac{K_D(P)}{K_D(T)} \quad (2)$$

$$\frac{[T]_{tot}}{[P]_{tot}} = \frac{[Cu]_{tot} - [Cu^{II}P]}{[P]_{tot}} + \frac{K_D(T)}{K_D(P)}\left(\frac{[Cu]_{tot}}{[Cu^{II}P]} - 1\right)\left(1 - \frac{[Cu^{II}P]}{[P]_{tot}}\right) \quad (3)$$

$$\frac{[Cu^{II}P]}{[P]_{tot}} = \frac{F_0 - F}{F_0 - F_1} \quad (4)$$

where $[Cu]_{tot}$ and $[P]_{tot}$ are the total Cu(II) and probe P concentrations and $F_0$, $F$, and $F_1$ are the respective fluorescence intensities at 550 nm when P binds no Cu(II), less than 1 equiv of Cu(II), and exactly 1 equiv of Cu(II). The protein targets do not emit fluorescence at 550 nm when excited at $\lambda_{ex}$ = 330 nm, so eqs 1−3 may be analyzed reliably by monitoring the response of the probe to Cu(II) binding. Then the term $[Cu^{II}P]$ may be determined directly via eq 4 and the Cu(II) affinity of the protein target expressed as $K_D(T)$ be estimated via curve fitting of the experimental data to eq 3 with the known probe affinity for Cu(II), $K_D(P)$.

Reaction 1 can be slow and may take >30 min to reach equilibrium, especially for those reactions involving molecules that bind Cu(II) in a so-called amino terminal copper and nickel (ATCUN) binding mode (Figure S3; *vide infra*).[32] Consequently, the experiments were conducted by preparing a series of solutions in an appropriate buffer that contained an equal concentration (2.0 $\mu$M) of the probe complex $Cu^{II}_x$−P ($x \leq 1.0$) and increasing concentrations of competing proteins to affect the competition. Each solution was incubated for >1.5 h until a stable fluorescence spectrum was reached and recorded. Stepwise recovery of the probe fluorescence with increasing protein concentration indicated Cu(II) transfer from the probe to the protein (eq 1), and the data were analyzed according to eqs 2−4.

The affinities of *Pf*-CopC for Cu(II) may be determined also via competition with classic Cu(II) ligands such as HEdta using the fluorescence emission of Trp77 as a detection probe ($\lambda_{ex}$ ∼ 280 nm; $\lambda_{em}$ ∼ 330 nm). The principle of the estimation is the same (eq 1−4), but, experimentally, a series of solutions containing an equal concentration (5.0 $\mu$M) of $Cu^{II}_x$−*Pf*-CopC ($x \leq 1.0$) and increasing concentrations of competing ligand (with known Cu(II) affinity) were prepared. It should be noted that the term $F_0$ in eq 4 in this case must be recorded for a solution containing the same concentration of $Cu^{II}_x$−CopC plus a large excess of a strong Cu(II) chelator such as Edta to ensure a complete removal of Cu(II) from the protein probe. The term $F_0$ defined in this way should be close to, but not necessary equal to, the fluorescence intensity of metal-free *apo*-CopC at the same concentration, due to a possible minor inner filter effect from other solution components. Such inner filter effects were shown previously to be negligible for DP probes at $\lambda_{em}$ ∼ 550 nm with $\lambda_{ex}$ ∼ 330 nm.[28]

The $K_D$ values for each protein were also determined at a range of pH values via competition with ligand HEdta and/or probes DP3 and DP4. The pH-dependent affinities of DP3 and DP4 were reported recently.[28] The pH-dependent affinities of HEdta were calculated via eq 5 from the published absolute dissociation constant ($K_D^{abs}$) and the proton ionization constants ($K_{an}$) of the amine functions[28,33]

$$K_D = K_D^{abs}(1 + \sum 10^{pK_{an} - npH}) \quad (n = 1-4) \quad (5)$$

The experiments were conducted in buffers (50 mM) Mes (pH 6.0−6.6), Mops (pH 7.0−7.4), Hepes (pH 7.8−8.2), and Ches (pH 8.5−9.2). On the other hand, the relationship between the determined $K_D$ and pH was also employed to model the most likely binding site using eq 5 to derive $K_D^{abs}$ for the Cu(II) complex and $K_{an}$ for the possible binding ligands.

**Analysis via Anion-Exchange Chromatography.** Binding of Cu(II) to *Pf*-CopC proteins may alter the net charge on the protein. This was analyzed via NaCl gradient elution of both the *apo* and $Cu^{II}$ forms in tandem from a home-packed analytical UNO Q anion-exchange column (1.0 mL; Bio-Rad) in Mops buffer (20 mM, pH 7.4). The identities of the eluted protein fractions were confirmed by ESI-MS and fluorescence quenching experiments (cf. Figure S1).



DOI: 10.1021/acs.inorgchem.5b00031
*Inorg. Chem.* 2015, 54, 2950−2959

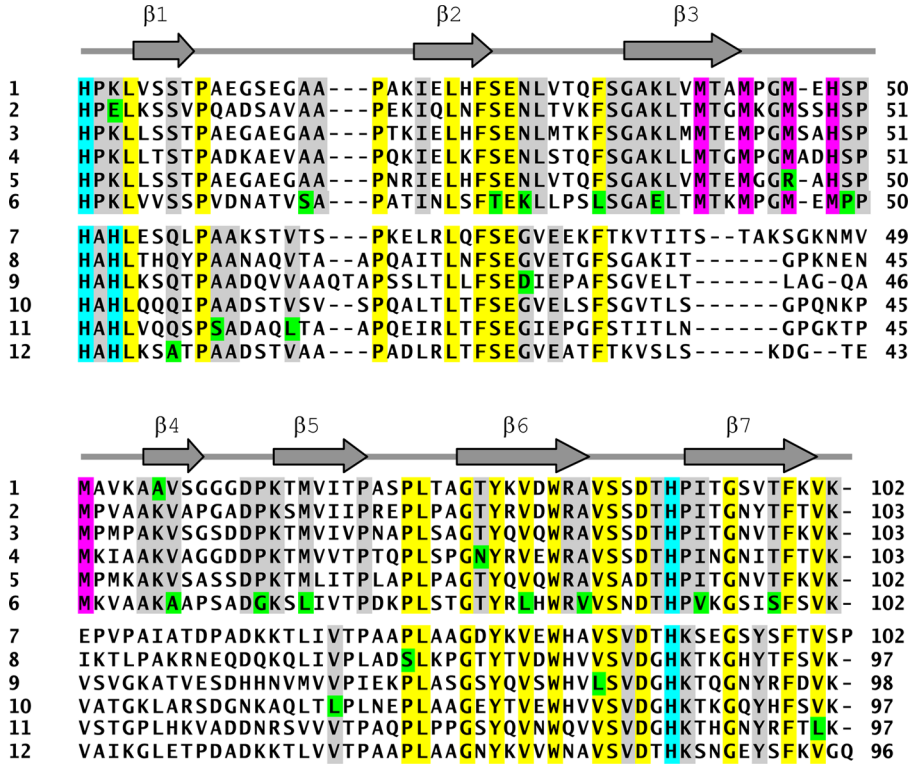


**Figure 1.** Multiple sequence alignment of Type A (1−6) and Type B (7−12) CopC proteins: (1) *Pseudomonas syringae* pathovar tomato CopC (accession no. aaa25808); (2) *Escherichia coli* PcoC (Q47454); (3) *Cupriavidus metallidurans* CH34 CopC (YP_581923); (4) *Pseudomonas putida* CopC (aap88297); (5) *Xanthomonas arboricola* pv juglandis CopC (Q56797); (6) *Pseudomonas fluorescens* CopC (WP_030140788); (7) *Pseudomonas syringae* CopC (WP_027898553); (8) *E. coli* CFT073 CopC (AAN80710); (9) *Dickeya zeae* CopC (WP_019845025); (10) *Enterobacter aerogenes* CopC (WP_026612268); (11) *Shimwellia blattae* CopC (WP_002445015); (12) *Pseudomonas fluorescens* SBW25 CopC (YP_002873498). Possible ligands for the Cu(I) and Cu(II) binding sites are highlighted in purple and teal, respectively. Conserved residues common to Types A and B are highlighted in yellow, whereas those restricted to each type are highlighted in gray. Single exceptions are shown in green. Secondary structural $\beta$-sheet elements as seen in the *P. syringae* CopC crystal structure (see Figure 2a) are shown above the aligned sequences.

## RESULTS

**Sequence Fingerprints of Type A and Type B CopC Proteins.** A protein BLAST search with either *Ec*-PcoC or *Pf*-CopC as a query sequence returned several hundred sequence homologues that may be divided into two distinct families, designated here as Type A and Type B (Figure 1). The Type A family includes those represented by the two well-characterized proteins, *Ec*-PcoC and *Ps*-CopC.[19,21,24,34−36] They feature a common $\beta$-barrel structure with separated binding sites specific for Cu(I) and Cu(II) (Figure 2a). The Cu(I) binding site is defined by a Met- and His-rich (4 Met, 1 His) binding loop for Cu(I), and the Cu(II) site is defined by a bidentate His1 (N-terminal amine; imidazole), a second His ligand plus a water, or an amino acid carboxylate side-chain ligand. They each exhibit subpicomolar affinities for their metal ion (Figures 1 and 2).[21,24]

The Type B family is represented by *Pf*-CopC and is present in more diverse microorganisms. It shares high sequence homology with Type A proteins (~40% identity and 60−70% similarity). A structural model of *Pf*-CopC, shown in Figure 2b, is based on a template of the known *apo-Ps*-CopC structure. Type B proteins are distinct in two aspects: (i) they lack a Cu(I) binding site and (ii) the potential Cu(II) binding site carries a so-called amino terminal copper and nickel (ATCUN) binding motif of the sequence $NH_2$-Xxx-Xxx-His that may constitute a tetragonal Cu(II) binding site that includes the N-terminal amine, the His3 side chain, and the two intervening

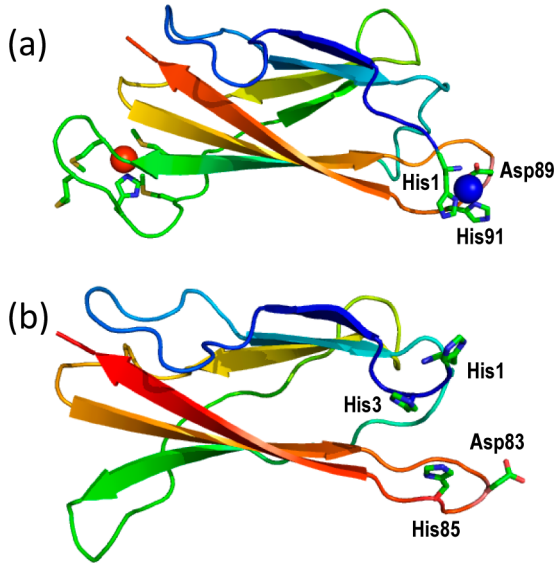


**Figure 2.** Copper binding sites in Types A and B CopC proteins. Identified or proposed side chain ligands are shown in stick representation. (a) X-ray crystal structure of $Cu^{I}Cu^{II}$−CopC from *P. syringae* (PDB code: 2C9Q): Cu(I), red; Cu(II), blue. (b) Structural model of *P. fluorescens* CopC based upon the NMR structure of *P. syringae apo*-CopC (PDB code: 1NM4) as a structural template.



DOI: 10.1021/acs.inorgchem.5b00031
*Inorg. Chem.* 2015, 54, 2950−2959

deprotonated peptide amides.[37] Consequently, the copper binding chemistry of Type B CopC proteins is expected to be different from that of Type A proteins. However, so far, none of the Type B proteins has been isolated for characterization in vitro. The present work expressed and isolated *Pf*-CopC as a representative example and undertook characterization of its copper binding chemistry. Four protein variants, H1F, H3K, H85F, and H1,85F, that target the expected Cu(II) binding site were generated to assist the characterization.

**Expression and Isolation of *Pf*-CopC Protein and Its Variants.** Synthetic genes for wild-type (wt) *Pf*-CopC and the four variants (including the leader sequence) were overexpressed in *E. coli* cells. The leader sequence was processed correctly to produce a mature protein with a native N-terminal His1 residue (or Phe1 for H1F). The expressed wt *Pf*-CopC protein exhibits a calculated pI of 6.3 and carries net charge of −1 at pH 7. Consequently, the expressed proteins may bind to either anion- or cation-exchange resin, depending on solution pH, but the respective affinities are expected to be weak. The ionic strength in the crude cell lysates was minimized to promote target protein binding to the chosen ion-exchange column. The procedures were tailored to the individual *Pf*-CopC proteins as detailed in the Experimental Section. All target proteins were isolated in high purity.

The CD spectrum of *Pf*-CopC (20 $\mu$M) in $KP_i$ buffer (5.0 mM, pH 7.4) was recorded and showed the anticipated fold, rich in $\beta$-sheet content (Figure S2b, red trace). The spectrum is similar to that of Type A *Ps*-CopC (Figure S2a), indicative of their similar protein fold. Mutation appears to induce some minor structural perturbations (Figure S2b).

**Affinity for Binding of Cu(I).** The isolated *Pf*-CopC proteins did not bind Cu(I) with appreciable affinity. A Cu(I) probe solution of $[Cu^{I}(Bca)_2]^{3-}$ (composition: $[Cu(I)]_{tot}$ = 30 $\mu$M, $[Bca]_{tot}$ = 80 $\mu$M) was prepared under anaerobic conditions in Mops buffer (50 mM, pH 7.4) containing dithionite (1.0 mM) as a strong reductant. Titration of *apo-Pf*-CopC (40 $\mu$M) into the above solution induced no detectable change in the solution absorbance at 562 nm, characteristic of the probe anion $[Cu^{I}(Bca)_2]^{3-}$ ($\varepsilon$ = 7900 $M^{-1}$ $cm^{-1}$; $\beta_2 = 10^{17.2}$ $M^{-2}$).[29] Under these conditions, Type A proteins compete with ligand Bca for Cu(I).[21,24]

**Stoichiometry and Affinity for Binding of Cu(II).** *Pf*-CopC and its four variants contain a Trp residue at position 77 that emits intense fluorescence at $\lambda_{max}$ = 335 nm with $\lambda_{ex}$ = 280 nm. Titration of each protein (5.0 $\mu$M) in Mops buffer (50 mM, pH 7.4) with $Cu^{2+}$ (200 $\mu$M) quenched the fluorescence intensity linearly with a sharp end point at 1 equiv of titrant (Figure S1). It is apparent that each of the five proteins binds 1 equiv of Cu(II) cleanly with high affinities.

Those affinities were determined in the pH range 6.0−9.2 with peptide probes DP3 and/or DP4 and were cross-checked with ligand HEdta using CopC Trp77 as a detection probe (see Experimental Section for details). Comparative experiments were conducted for Type A proteins *Ec*-PcoC and *Ps*-CopC, whose affinities have been reported previously.[21,24,28] The results are summarized in Table 1 and Figures 3, 4, and S4.

At pH 7.4, each of the five *Pf*-CopC proteins competed strongly for Cu(II) with the DP4 probe (Figure 3a), indicating competitive affinities in the femtomolar range. The experimental data (including comparative data for Type A proteins *Ec*-PcoC and *Ps*-CopC) was processed according to eq 1−4 and was based on the reported affinity of DP4 for Cu(II) at pH 7.4 (log $K_D$ = −14.1).[28] The derived affinities (expressed as p$K_D$ = −log $K_D$) decreased in the following order

**Table 1. Conditional Dissociation Constants (Log $K_D$) for Cu(II) Complexes of *Pf*-CopC Proteins and Related Peptides and Proteins Determined via Ligand Competition[a]**

| | log $K_D$ | | | | |
|---|---|---|---|---|---|
| protein/peptide | pH 6.2 (Mes) | pH 7.4 (Mops) | pH 9.2 (Ches) | probe/ competing ligand | ref |
| *Pf*-CopC | −13.3 | −15.5 | −17.1 | DP4 | this work |
| | | −15.6 | −17.0 | CopC/ HEdta | this work |
| *Pf*-CopC H1F | −10.7 | −13.9 | | DP3 | this work |
| | −10.7 | −13.9 | −16.9 | DP4 | this work |
| *Pf*-CopC H3K | −11.3 | | | DP3 | this work |
| | −11.4 | −14.1 | −17.0 | DP4 | this work |
| *Pf*-CopC H85F | −11.8 | | | DP3 | this work |
| | −11.9 | −14.6 | −17.0 | DP4 | this work |
| *Pf*-CopC H1/85F | −10.0 | −13.6 | | DP3 | this work |
| | −10.0 | −13.6 | −16.8 | DP4 | this work |
| *Ps*-CopC | | | −14.4 | DP3 | this work |
| | −12.3 | −13.7 | | DP4 | this work |
| *Ec*-PcoC | −11.3 | −13.5 | −14.0 | DP3 | 28 |
| | −11.5 | −13.5 | | DP4 | 28 |
| *Ec*-PcoC-H1F | | −8.2 | | DP1 | 28 |
| GHK | −10.4 | −13.3 | −16.3 | DP4 | 28 |
| DAHK | −10.0 | −13.8 | −17.7 | DP4 | 28 |
| DP3 | −10.1 | −12.3 | −13.4 | DP3/Gly-His | 28 |
| DP4 | −11.1 | −14.1 | −18.0 | DP4/His-Egta | 28 |
| HEdta | −13.7 | −14.9 | −16.7 | | 33 |

[a]See Figure 3 for general experimental conditions.

$$Pf\text{-CopC (15.5)} > \text{H85F (14.6)} > \text{H3K (14.1)} > \text{H1F (13.9)} > \text{H1/85F (13.6)} \sim Ps\text{-CopC (13.7)} \sim Ec\text{-PcoC (13.5)} \gg Ps\text{-CopC-H1F} \sim Ec\text{-PcoC-H1F (8.2)} \quad (6)$$

Wild-type *Pf*-CopC exhibits subfemtomolar affinity. The estimate was confirmed independently via competition with the classic Cu(II) ligand, HEdta, using Trp77 as a fluorescent probe. The affinity of HEdta at pH 7.4 closely matches that of *Pf*-CopC (p$K_D$ = 14.9 vs 15.5; see Table 1 and Figure S4).

As expected, the $K_D$ values for both types of proteins vary with solution pH (Figure 4). The experimental relationships were fitted satisfactorily to eq 5 (Figure 4a) on the basis of the Cu(II) sites anticipated for the two classes (see Figure 7a,b; Type A site: one N-terminal amine, two His side chains, and a carboxylate; Type B site: one N-terminal amine and three His side chains). The same curve-fitting procedure was applied satisfactorily to the DP3 probe (Figure 4a) that binds Cu(II) with one N-terminal nitrogen and three His side-chain imidazole groups (see Figure 7g).[28] The derived parameters log $K_D^{abs}$ (i.e., the pH-independent dissociation constant) for the


DOI: 10.1021/acs.inorgchem.5b00031
*Inorg. Chem.* 2015, 54, 2950−2959

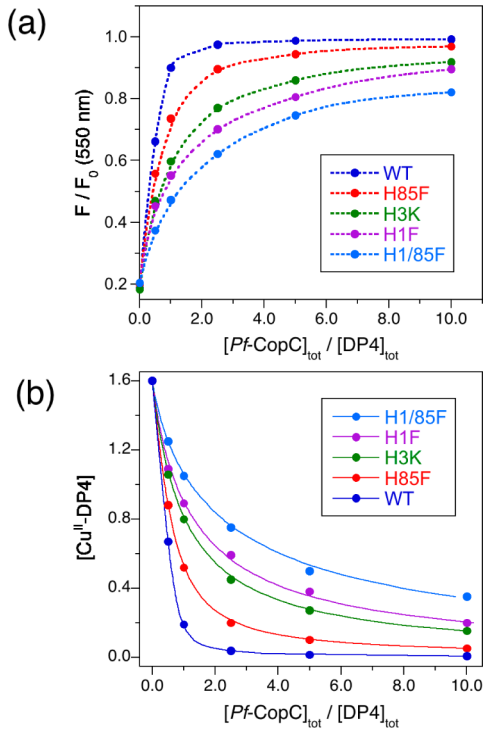


**Figure 3.** Determination of conditional $K_D$ for *Pf*-CopC proteins with fluorescent probe DP4 in Mops buffer (50 mM, pH 7.4): (a) recovery of the Cu(II)-quenched fluorescence intensity of $Cu^{II}_{0.8}$–DP4 (2.0 $\mu$M) upon titration with each *Pf*-CopC protein; (b) correlation of $[Cu^{II}–DP4]$ versus $[CopC]_{tot}/[DP4]_{tot}$, where the solid traces are the fits of the experimental data to eq 3, allowing estimation of conditional $K_D$ values (see Table 1).

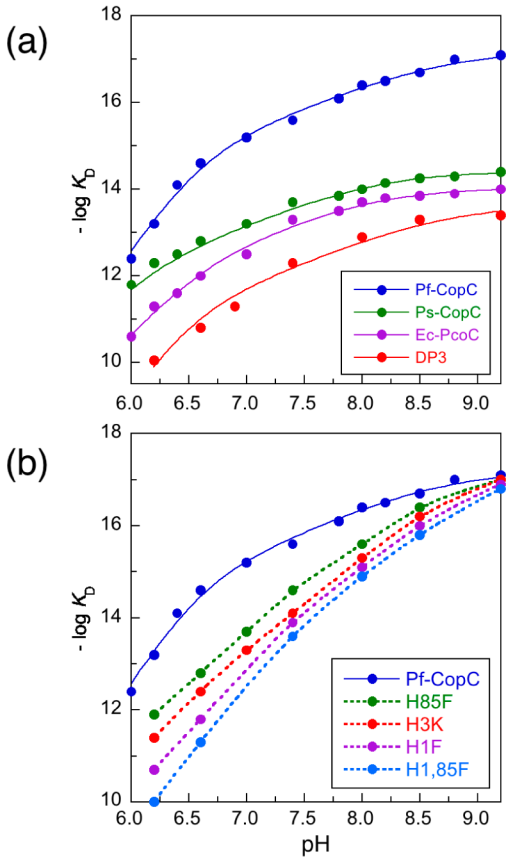


**Figure 4.** Variation of Cu(II) conditional dissociation constant $pK_D$ (= $-\log K_D$) with solution pH for: (a) *Pf*-CopC, *Ps*-CopC, *Ec*-PcoC, and probe DP3; (b) *Pf*-CopC and its variants. The solid traces show the fits of the experimental data to eq 5; derived parameters are listed in Table 2. The dotted traces are the simple interpolation of the experimental data points since the data cannot be fitted with eq 5.

Cu(II) complexes and the $pK_a$ values for the N-terminal nitrogen and for the His side-chain imidazole nitrogen are listed in Table 2 and are within the expected ranges.

Mutation of His3 in *Pf*-CopC to the conserved Lys3 present in Type A proteins generated a protein variant, H3K, whose affinity is higher than those of Type A by a factor of 3 at pH 7.4 and whose $K_D$ is more sensitive to pH than are those of Type A proteins (Table 1 and Figure 4b). Mutation of proposed ligand His85 to the noncoordinating Phe also decreased the Cu(II) affinity and increased the pH sensitivity of variant H85F (Table 1 and Figure 4b). In fact, the pH dependences for both protein variants H3K and H85F cannot be fitted to eq 5. It would appear that at least one ligand with $pK_a > 9.2$ is involved in the binding site (*vide infra*).

Mutation of His1 to Phe1 decreased the Cu(II) affinity by 1.6 orders of magnitude at pH 7.4, and the decrease becomes smaller at higher pH values (Table 1 and Figure 4b). The same trend applies to the double mutant, H1,85F, in which both His1 and His85 are converted to Phe: the affinity decreases marginally from that of H1F but does not essentially alter the pH dependence (Table 1 and Figure 4b). The pH dependencies for these two protein variants cannot be fitted with eq 5 either within the pH range 6.0–9.2.

**Spectroscopic Characterization.** The *d*–*d* solution spectra of the Cu(II) complexes of all five *Pf*-CopC proteins are displayed in Figure 5, together with those of two peptides, GHK and DAHK, whose Cu(II) binding sites have been well-documented.[38] The data are summarized in Table S2 and include those for the Type A protein *Ec*-PcoC and the Cu(II) probes DP3 and DP4.[21,28] The *d*–*d* transitions for wt *Pf*-CopC and its two variants, H3K and H85F, are similar with maximum absorbance between 580 and 585 nm and molar extinction coefficients in the range 145–170 $M^{-1}$ $cm^{-1}$. Similar observations hold for *Ec*-PcoC and in peptides DP3 and GHK, whose absorption maxima lie at slightly longer wavelengths (600–625 nm). On the other hand, the absorptions of the Cu(II) complexes of variants H1F and H1,85F undergo a blue shift of ~60, to 530 nm.

Each $Cu^{II}$–*Pf*-CopC protein has an EPR spectrum characteristic of a Type II copper center of pseudoaxial symmetry and exhibits similar EPR parameters ($g_{\|}$ = ~2.25, $A_{\|}$ = ~179G, and $g_{\perp}$= ~2.05; Table S2 and Figure S5). The overall spectra of Types A and B $Cu^{II}$–CopC proteins are similar and show clear

**Table 2. Thermodynamic Data of Cu(II) Sites Derived from Correlation of Log $K_D$ and pH[a]**

| protein | Cu(II) binding site | log $K_D^{abs}$ | $pK_a$ ($NH_2$) | $pK_a$ ($N^{im}$) |
|---|---|---|---|---|
| *Pf*-CopC | $NH_2$ (H1); 3 $N^{Im}$ (H1,3,85) | −17.2 | 8.8 | 6.6 |
| *Ps*-CopC | $NH_2$ (H1); 2 $N^{Im}$ (H1,91); $COO^-$ (D89) | −14.4 | 8.2 | 6.1 |
| *Ec*-PcoC | $NH_2$ (H1); 2 $N^{Im}$ (H1,92); $COO^-$ (D90) | −14.0 | 8.2 | 6.5 |
| DP3 peptide | $NH_2$ (H1); 3 $N^{Im}$ (H1,5,7) | −13.6[b] | 8.8[b] | 6.5[b] |

[a]See Figure 4a for experiments; parameters obtained by fitting to eq 5. [b]The data was taken from ref 28.



DOI: 10.1021/acs.inorgchem.5b00031
*Inorg. Chem.* 2015, 54, 2950–2959

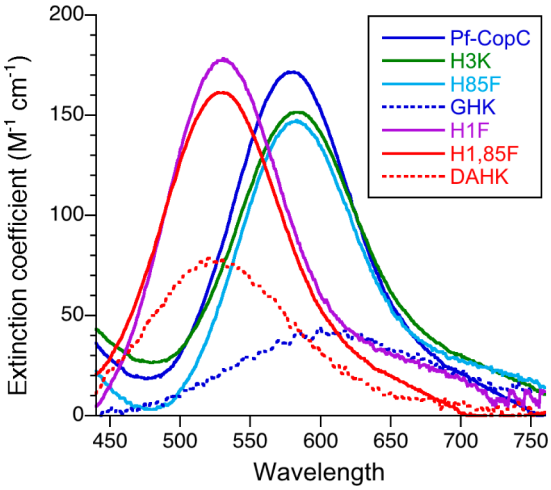


**Figure 5.** Solution spectra of Cu(II) complexes of *Pf*-CopC proteins and peptides GHK and DAHK in Mops buffer (50 mM, pH 7.4). The *d*−*d* transition around 525 nm is a fingerprint of the Cu(II) center in the ATCUN binding mode and is seen in the H1F and H1,85F proteins and in DAHK peptide.

superhyperfine splitting in the perpendicular component attributable to the coupling of $^{63}$Cu/$^{65}$Cu ($I = {}^{3}/_{2}$) to more than one $^{14}$N nucleus ($I = 1$). The coupling is best resolved for *Pf*-CopC, where a nine-line superhyperfine splitting was apparent (Figures S5b and S6a), consistent with a 4N binding site. A similar nine-line superhyperfine pattern is visible for variant H3K (Figures S5c and S6b). Spectra of the other variants are less well-resolved but are consistent with the presence of multiple N-based ligands.

**Analysis via Ion-Exchange Chromatography.** The isoelectric points (pI) of the five *Pf*-CopC proteins produced in this work were estimated to be <7.0 with low net anionic charges: the *apo* forms bound weakly to an anion-exchange UNO-Q column at pH 7.4 (Table 3 and Figure 6). Binding of

**Table 3. Analysis of Cu(II) Binding via an Anion-Exchange UNO-Q Column**[a]

| entry in Figure 6 | protein or peptide | pI | net charge at pH 7.4 | elution position at [NaCl] (mM)[b] | Δ[NaCl] (mM) upon $Cu^{II}$ binding |
|---|---|---|---|---|---|
| a | *apo*-*Pf*-CopC | 6.3 | −1 | 111 | 11 |
| | $Cu^{II}$−*Pf*-CopC | >6.3 | >−1 | 100 | |
| b | *apo*-H85F | 6.1 | −1 | 112 | 11 |
| | $Cu^{II}$−H85F | >6.1 | >−1 | 101 | |
| c | *apo*-H3K | 6.9 | 0 | 98 | 3 |
| | $Cu^{II}$−H3K | ~6.9 | ~0 | 95 | |
| d | *apo*-DP3 probe | 5.7 | −2 | 86 | 15 |
| | $Cu^{II}$−DP3 probe | >5.7 | >−2 | 71 | |
| e | *apo*-H1F | 6.1 | −1 | 113 | − 5 |
| | $Cu^{II}$−H1F | <6.1 | <−1 | 118 | |
| f | *apo*-H1,85F | 5.7 | −1 | 122 | − 7 |
| | $Cu^{II}$−H1,85F | <5.7 | <−1 | 129 | |
| g | *apo*-DP4 probe | 7.0 | 0 | 76 | − 10 |
| | $Cu^{II}$−DP4 probe | <7.0 | <0 | 86 | |

[a]In Mops buffer (20 mM, pH 7.4) with a NaCl gradient of 0−200 mM. [b]The elution position of each protein varied slightly with different FPLC settings and buffer preparations, but the relative positions of different samples were constant when eluted in tandem under the same conditions.

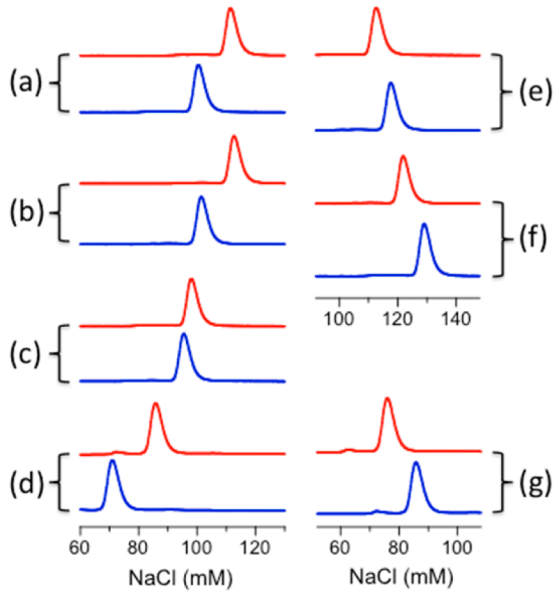


**Figure 6.** Relative elution positions of *apo* (in red) and Cu(II) forms (in blue) of proteins and peptides from an UNO-Q anion-exchange column (1.0 mL; Bio-Rad) in Mops buffer (20 mM, pH 7.4; NaCl gradient 0−300 mM): (a) *Pf*-CopC, (b) H85F, (c) H3K, (d) control peptide probe DP3, (e) H1F, (f) H1/85F, and (g) control peptide probe DP4.

Cu(II) to these proteins is expected to alter the individual protein isoelectric points in a way that depends on the nature of the individual binding sites. This effect was analyzed via comparative elution of both the *apo* and $Cu^{II}$ forms from an analytical anion-exchange column under the same conditions.

Binding of Cu(II) to *apo*-*Pf*-CopC causes earlier elution by ~11 mM NaCl (Table 3 and Figure 6a), suggesting that binding of the ion leads to a net gain in positive charge. Similar earlier elution upon Cu(II) binding was observed for variant H85F and probe DP3, but binding of Cu(II) to variant H3K induced little change in elution position (Table 3 and Figure 6b−d). In contrast, binding of Cu(II) to either variant H1F or H1,85F induced later elution from the anion-exchange column, as was also the case for probe DP4 (Table 3 and Figure 6e−g).

## DISCUSSION

**A Novel Cu(II) Site in Type B CopC Proteins.** *Pf*-CopC belongs to a new family of CopC proteins, designated Type B in this work. They differ from the two well-characterized homologues, *Ec*-PcoC and *Ps*-CopC, of Type A. The latter possess two separated copper-binding sites that are specific for Cu(I) and Cu(II), whereas the former possess one high-affinity Cu(II) site and lack a Cu(I) site. Sequence alignments predict that the Cu(II) sites in Type B may be different from those in Type A (Figure 1). The latter bind Cu(II) with a ligand set of 3N + O, as shown in Figure 7a (Table 2).[21,24] The present work presents initial isolation and characterization data for a Type B protein, *Pf*-CopC.

A range of variants of *Pf*-CopC targeting the predicted Cu(II) site was generated. The data demonstrate that this protein features a Cu(II) binding site that is distinctly different from that of Type A proteins and possesses some unusual binding properties. Like the Type A proteins *Ec*-PcoC and *Ps*-CopC,[21,24] *Pf*-CopC features a His residue at position 1 that may act as a bidentate ligand for Cu(II). However, unlike those


DOI: 10.1021/acs.inorgchem.5b00031
*Inorg. Chem.* 2015, 54, 2950−2959

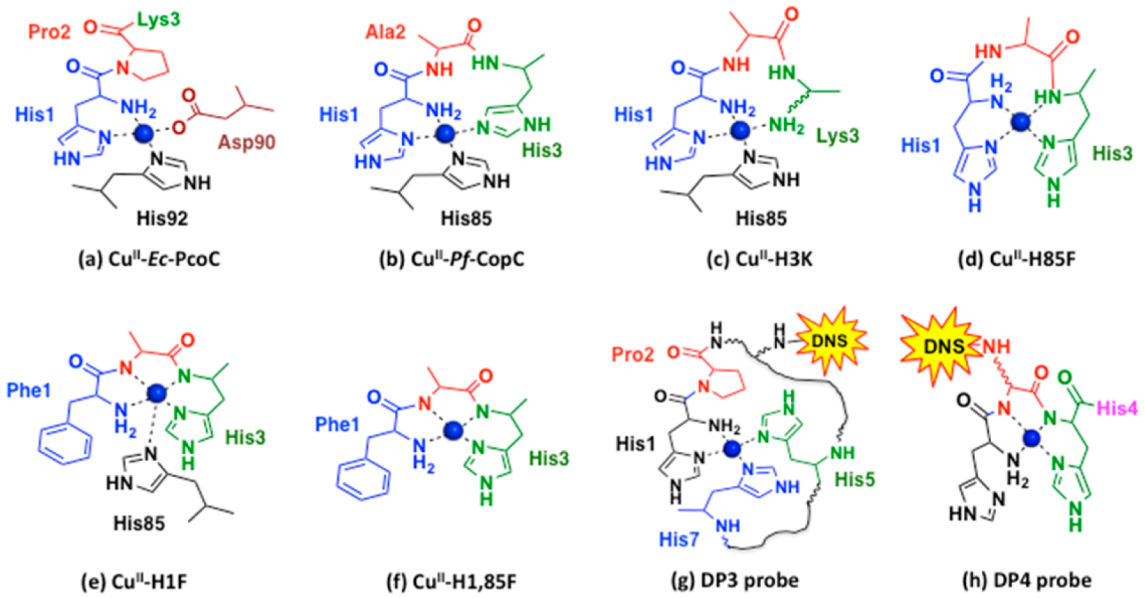


**Figure 7.** Proposed Cu(II) centers in Cu(II) complexes of *Ec*-PcoC and *Pf*-CopC (plus its variants). Those for probes DP3 and DP4 have been discussed previously.[28] The Cu(II) atom is represented by a blue sphere. DNS represents the fluorescent dansyl group attached to Lys.

analogues, *Pf*-CopC also features a His residue at position 3 that has the potential to enforce an ATCUN binding mode involving His3, the N-terminal amine, and the two deprotonated peptide backbone amides at positions 2 and 3 as co-ligands.[37] Such Cu(II) binding sites are common in several systems, such as the peptides HKHH (DP4; Figure 7h) and DAHK (Table 1) and serum albumins, proposed to be important for transport of Cu(II) in blood.[28,37,38] The high energy cost of deprotonation of the two peptide amide ligands is compensated by the formation of three favorable chelate rings of 6, 5, and 6 members (Figure 7h).

However, the ATCUN binding mode is not compatible with His1 as a bidentate ligand, as the backbone amides at positions 2 and 3 are then not available for steric reasons. This work demonstrates that the Cu(II) site in *Pf*-CopC adopts a non-ATCUN binding mode employing His1 as a bidentate ligand and both His3 and His85 side chains as the two co-ligands (Figure 7b), but upon mutation of the key ligand His1, the ATCUN binding mode is adopted (Figure 7e,f). The evidence is outlined below (with controls provided by several well-characterized proteins (*Ps*-CopC and *Ec*-PcoC of Type A and serum albumins)[21,24,37] and peptides (GHK, DAHK, HPKDHDH (DP3), and HKHH (DP4))).[28,38]

*(i) The Magnitude of the Binding Affinity for Cu(II) (Figure 4 and Table 1).* The affinity of Type B protein *Pf*-CopC is 2 orders of magnitude higher than those of Type A proteins such as *Ps*-CopC and *Ec*-PcoC at pH 7.4 (eq 6). This may be attributed to the His3 ligand, available in Type B but not in Type A proteins (Figure 1). In addition, conversion of the conserved and rigid Pro2 in Type A to the conserved but flexible Ala2 in the Type B proteins (Figure 1) may be influential, consistent with the observation that mutation of His3 to the conserved Lys3 in Type A proteins does not convert the site from Type B to Type A (*vide infra*).

*(ii) pH Dependency of the Binding Affinity (Figure 4 and Table 2).* The experimental relationships were fitted satisfactorily to eq 5 based on the Cu(II) binding sites anticipated above for the two classes. Type A proteins *Ps*-CopC and *Ec*-PcoC feature an N-terminal amine, two His, and a carboxylate as ligands (Figure 7a), whereas Type B example *Pf*-CopC and the control peptide probe DP3[28] are proposed to each employ an N-terminal amine and three His ligands (Figure 7b,g). In contrast, we demonstrated recently that the pH−affinity relationships for control peptides DAHK and HKHH (DP4) cannot be fitted to eq 5 within the pH window 6.2−9.2.[28] They both bind Cu(II) in an ATCUN mode comprising one N-terminal amine, one His side chain, and two peptide bond amides (cf. Figure 7h) where the two amide ligands are highly basic with $pK_a \gg 9.2$.[28,38] Apparently, the Cu(II) site in *Pf*-CopC does not adopt the ATCUN binding mode.

*(iii) Spectroscopic Fingerprints (Figures 5, S5, and S6 and Table S2).* The *d*−*d* transitions for the Cu(II) complex of wt *Pf*-CopC exhibit an absorption maximum around 580 nm. Those of other non-ATCUN molecules such as Type A CopC protein *Ec*-PcoC and peptides DP3 and GHK show similar absorption maxima at slightly longer wavelengths (600−625 nm; Table S2). In contrast, the *d*−*d* transition maxima for the Cu(II) complexes of the two control peptide ligands, DAHK and HKHH (DP4), occur at ∼525 nm,[28,38] a position regarded as a fingerprint for the ATCUN binding mode.[37] Likewise, the solution spectra of serum albumins feature similar absorption maxima at ∼525 nm, attributable to the presence of a Cu(II) ATCUN center in these proteins.[37] This, again, suggests that *Pf*-CopC binds Cu(II) in a non-ATCUN mode.

The EPR spectrum of the Cu(II) form of *Pf*-CopC shows a clear nine-line superhyperfine splitting pattern for the perpendicular component, attributable to the coupling of $^{63}$Cu/$^{65}$Cu ($I = {}^3/_2$) to four $^{14}$N nucleus ($I = 1$) (Figures S5b and S6a). This is consistent with a 4N binding site proposed in Figure 7b.

*(iv) Change in Net Protein Charge upon Cu(II) Binding (Figure 6 and Table 3).* Binding of Cu(II) to *apo*-*Pf*-CopC leads to a net gain in positive charge (Figure 6a and Table 3). At pH 7.4, the N-terminal nitrogen of the *apo* protein will be protonated, whereas the His side chains will be neutral. Binding of Cu(II) to such a site would result in a loss of the N-terminal ammonium proton only with a net gain of one positive unit of overall charge due to formation of the proposed [Cu$^{II}$(NH$_2$-



DOI: 10.1021/acs.inorgchem.5b00031
*Inorg. Chem.* 2015, 54, 2950−2959

)($N^{Im}$-His)$_3$]$^{2+}$ site (Figure 7b). Likewise, a net gain in positive charge was detected for DP3 probe peptide (Figure 6d) that features a comparable Cu(II) site (Figure 7g)[28] and for Type A proteins *Ec*-PcoC and *Ps*-CopC that were previously demonstrated to possess a Cu(II) site of [$Cu^{II}$($NH_2$-)($N^{Im}$-His)$_2$($^-$OOC−)]$^+$ (Figure 7a).[21,24] In contrast, binding of Cu(II) to the ATCUN peptide HKHH (DP4) leads to a net gain in negative (instead of positive) charge (Figure 6g).

In conclusion, the combined evidence supports the presence of a novel Cu(II) site in *Pf*-CopC, as shown in Figure 7b. Intriguingly, the similar Cu(II) binding motif HKHH for probe DP4 was demonstrated to bind Cu(II) in the ATCUN binding mode (Figure 7h)[28] rather than in the binding modes as seen in *Pf*-CopC that employ His1 as a bidentate ligand (Figure 7b). This highlights the important caveat that the metal binding motif of a short peptide may not mimic reliably a similar N-terminal metal binding motif in a folded protein, as seen also in some other cases.[39] A metal site in a flexible short peptide is usually dominated by the requirements of the metal coordination sphere, whereas a metal site in a protein will inevitably be constrained by the protein fold.

**Cu(II) Sites in Protein Variants H3K and H85F.** One of the major differences between the two types of CopC protein lies in the third residue that is a conserved Lys for Type A and a conserved His for Type B. In an attempt to convert the Cu(II) site from Type B to Type A, the His3 in *Pf*-CopC was mutated to Lys3. However, the Cu(II) site in *Pf*-CopC H3K variant has proven to be distinctly different from that in Type A CopC: the Cu(II) affinity of H3K is highly dependent on pH, and the relationship cannot be modeled with eq 5 within the pH range 6.2−9.2 (Figure 4b). This suggests that the Cu(II) binding site in H3K involves at least one highly basic ligand with p$K_a$ > 9.2, such as the Lys3 side chain and/or backbone amide(s). The following observations favor a Lys3 coordination mode as shown Figure 7c: (i) the *d*−*d* transition maximum for the solution spectrum of Cu(II)−H3K occurs at 585 nm, not 525 nm (Figure 5); (ii) binding of Cu(II) to H3K induced little change in its affinity for an ion-exchange column (Figure 6c); (iii) a nine-line superhyperfine splitting pattern for EPR of Cu(II)−H3K is apparent, consistent with a 4N metal site (Figure S6b). However, Lys3 in Type A is not involved in Cu(II) binding, probably due to the rigidity of the Pro2 residue in Type A rather than the flexible Ala2 in Type B (Figure 1).

Mutation of ligand His85 to the noncoordinating side chain of Phe also decreased the Cu(II) affinity and increased the pH dependency of variant H85F (Table 1 and Figure 4b). The overall evidence (Figures 5 and S6; Figure 6b vs 6e−g) favors the structure of Figure 7d.

**Cu(II) Sites in Protein Variants H1F and H1,85F.** Mutation of His1 to Phe1 for Type A CopC perturbs Cu(II) binding dramatically with an affinity decrease by more than 5 orders of magnitude (Table 1).[21,24,28] In contrast, the same mutation for Type B *Pf*-CopC leads to a modest decrease of 1.6 order of magnitude at pH 7.4, and that decrease becomes even smaller with increasing pH (Table 1 and Figure 4b). Further mutation of His85 to Phe only decreases the Cu(II) affinity of H1,85F variant marginally, suggesting a minor contribution of His85 to the Cu(II) binding site in the H1F protein, most likely as an axial ligand. This evidence suggests that His1 mutation leads to a conversion of the Cu(II) binding in *Pf*-CopC from a His1 bidentate mode to an ATCUN binding mode. The following observations support this conclusion: (i) the Cu(II) affinities of both H1F and H1,85F vary considerably with pH, and the relationships cannot be fitted with eq 5 within the pH range 6.0−9.2, consistent with the backbone amide(s) (p$K_a$ > 9.2) being involved in Cu(II) binding (Figure 4b); (ii) both complexes $Cu^{II}$−H1F and $Cu^{II}$−H1,85F exhibit *d*−*d* transitions with a maximum at 530 nm, characteristic of an ATCUN Cu(II) center in all related complexes (Figure 5 Table S2, and ref 37); (iii) binding of Cu(II) to the *apo* form of either proteins results in a net gain in protein negative charge at pH 7.4 (Figure 6e,f), consistent with deprotonation of more than two ligands of the Cu(II) binding sites. Several well-documented ATCUN Cu(II) centers, such as those in peptides DAHK and HKHH (the DP4 probe) and in various serum albumin proteins, display similar characters (Figure 5 and Figure 6g and refs 28 and 37). Consequently, the Cu(II) sites in H1F and H1,85F are established as those depicted in Figure 7e,f, respectively. Apparently, the presence of His1 as a bidentate ligand in *Pf*-CopC plays a pivotal role in disfavoring the ATCUN binding mode. Interestingly, the Cu(II) site in the double mutant, H1,85F, may be taken as a pure contribution from the ATCUN motif $NH_2$-Xxx-Xxx-His in *Pf*-CopC (Figure 7f), and its Cu(II) affinity lies below all that of other CopC forms generated in this work within the pH range 6.0−9.2 (Figure 4b). Consequently, it can be concluded that additional Cu(II) ligands constrained to specific positions by the folded protein structure can modulate the basic ATCUN mode to thermodynamically more favorable forms.

Type B CopC proteins belong to a large protein family and prevail in a wide range of microorganisms. However, their biological functions remain essentially unexplored. The single functional study for these proteins was reported in 2008 for *Pf*-CopC.[25] The present work demonstrates that the periplasmic protein *Pf*-CopC features a novel Cu(II) binding site with affinity 2 orders of magnitude higher than that in known Type A proteins. The increased Cu(II) affinity is consistent with its proposed functional role of sequestration of periplasmic copper under copper-limiting conditions.

## ■ ASSOCIATED CONTENT

### Supporting Information

ESI-QTOF-MS data for the purified proteins (Table S1), spectroscopic data for Cu(II) complexes (Table S2), fluorescence titration of *Pf*-CopC proteins (Figure S1), CD spectrum (Figure S2), Cu(II)-exchange kinetics (Figure S3), determination of Cu(II) $K_D$ with HEdta (Figure S4), and EPR spectra (Figures S5 and S6). This material is available free of charge via the Internet at http://pubs.acs.org.

## ■ AUTHOR INFORMATION

### Corresponding Author

*E-mail: z.xiao@unimelb.edu.au. Tel: +61 3 9035 6072. Fax: +61 3 9347 5180.

### Notes

The authors declare no competing financial interest.

## ■ ACKNOWLEDGMENTS

This work was supported by funding from Australian Research Council grant DP130100728. We thank Sioe See Volaric (University of Melbourne) for providing technical support for recording EPR spectra.



DOI: 10.1021/acs.inorgchem.5b00031
*Inorg. Chem.* 2015, 54, 2950−2959

## REFERENCES


(1) Arguello, J. M.; Raimunda, D.; Padilla-Benavides, T. *Front. Cell. Infect. Microbiol.* **2013**, *3*, 73.
(2) Rensing, C.; McDevitt, S. F. *Met. Ions Life Sci.* **2013**, *12*, 417−50.
(3) Bondarczuk, K.; Piotrowska-Seget, Z. *Cell Biol. Toxicol.* **2013**, 1−9.
(4) Lutsenko, S. *Curr. Opin. Chem. Biol.* **2010**, *14*, 211−17.
(5) Robinson, N. J.; Winge, D. R. *Annu. Rev. Biochem.* **2010**, *79*, 537−62.
(6) Tottey, S.; Patterson, C. J.; Banci, L.; Bertini, I.; Felli, I. C.; Pavelkova, A.; Dainty, S. J.; Pernil, R.; Waldron, K. J.; Foster, A. W.; Robinson, N. J. *Proc. Natl. Acad. Sci. U.S.A* **2012**, *109*, 95−100.
(7) Rensing, C.; Grass, G. *FEMS Microbiol. Rev.* **2003**, *27*, 197−213.
(8) Roberts, S. A.; Wildner, G. F.; Grass, G.; Weichsel, A.; Ambrus, A.; Rensing, C.; Montfort, W. R. *J. Biol. Chem.* **2003**, *278*, 31958−63.
(9) Djoko, K. Y.; Chong, L. X.; Wedd, A. G.; Xiao, Z. *J. Am. Chem. Soc.* **2010**, *132*, 2005−15.
(10) Cortes, L.; Wedd, A. G.; Xiao, Z. *Metallomics* **2015**, DOI: 10.1039/C5MT00001G.
(11) Grass, G.; Rensing, C. *Biochem. Biophys. Res. Commun.* **2001**, *286*, 902−8.
(12) Franke, S.; Grass, G.; Rensing, C.; Nies, D. H. *J. Bacteriol.* **2003**, *185*, 3804−12.
(13) Long, F.; Su, C. C.; Zimmermann, M. T.; Boyken, S. E.; Rajashankar, K. R.; Jernigan, R. L.; Yu, E. W. *Nature* **2010**, *467*, 484−8.
(14) Su, C.-C.; Long, F.; Zimmermann, M. T.; Rajashankar, K. R.; Jernigan, R. L.; Yu, E. W. *Nature* **2011**, *470*, 558−62.
(15) Su, C. C.; Long, F.; Yu, E. W. *Protein Sci.* **2011**, *20*, 6−18.
(16) Chacón, K. N.; Mealman, T. D.; McEvoy, M. M.; Blackburn, N. J. *Proc. Natl. Acad. Sci. U.S.A* **2014**, *111*, 15373−78.
(17) Outten, F. W.; Huffman, D. L.; Hale, J. A.; O'Halloran, T. V. *J. Biol. Chem.* **2001**, *276*, 30670−7.
(18) Rouch, D. A.; Brown, N. L. *Microbiology* **1997**, *143*, 1191−202.
(19) Huffman, D. L.; Huyett, J.; Outten, F. W.; Doan, P. E.; Finney, L. A.; Hoffman, B. M.; O'Halloran, T. V. *Biochemistry* **2002**, *41*, 10046−55.
(20) Djoko, K. Y.; Xiao, Z.; Wedd, A. G. *ChemBioChem* **2008**, *9*, 1579−82.
(21) Djoko, K. Y.; Xiao, Z.; Huffman, D. L.; Wedd, A. G. *Inorg. Chem.* **2007**, *46*, 4560−68.
(22) Zimmermann, M.; Udagedara, S. R.; Sze, C. M.; Ryan, T. M.; Howlett, G. J.; Xiao, Z.; Wedd, A. G. *J. Inorg. Biochem.* **2012**, *115*, 186−97.
(23) Lee, S. M.; Grass, G.; Rensing, C.; Barrett, S. R.; Yates, C. J.; Stoyanov, J. V.; Brown, N. L. *Biochem. Biophys. Res. Commun.* **2002**, *295*, 616−20.
(24) Zhang, L.; Koay, M.; Maher, M. J.; Xiao, Z.; Wedd, A. G. *J. Am. Chem. Soc.* **2006**, *128*, 5834−50.
(25) Zhang, X. X.; Rainey, P. B. *Environ. Microbiol.* **2008**, *10*, 3284−94.
(26) Cha, J. S.; Cooksey, D. A. *Appl. Environ. Microbiol.* **1993**, *59*, 1671−74.
(27) Cooksey, D. A. *FEMS Microbiol. Rev.* **1994**, *14*, 381−6.
(28) Young, T. R.; Wijekoon, C. J. K.; Spyrou, B.; Donnelly, P. S.; Wedd, A. G.; Xiao, Z. *Metallomics* **2015**, DOI: 10.1039/C4MT00301B.
(29) Xiao, Z.; Brose, J.; Schimo, S.; Ackland, S. M.; La Fontaine, S.; Wedd, A. G. *J. Biol. Chem.* **2011**, *286*, 11047−55.
(30) Larkin, M. A.; Blackshields, G.; Brown, N. P.; Chenna, R.; McGettigan, P. A.; McWilliam, H.; Valentin, F.; Wallace, I. M.; Wilm, A.; Lopez, R.; Thompson, J. D.; Gibson, T. J.; Higgins, D. G. *Bioinformatics* **2007**, *23*, 2947−8.
(31) Kiefer, F.; Arnold, K.; Kunzli, M.; Bordoli, L.; Schwede, T. *Nucleic Acids Res.* **2009**, *37*, D387−92.
(32) Titration of $CuSO_4$ solution into either peptide probe or protein solution generally induced fast and quantitative binding of Cu(II) to most target molecules except when the target molecule only binds Cu(II) weakly. However, the Cu(II)-exchange of eq 1 may be slow, especially for those Cu(II) binding molecules adopting an ATCUN binding mode (cf. Figure S3). This is likely due to limiting free $Cu_{aq}^{2+}$ concentrations under the Cu(II)-exchange conditions and the involvement of protonation and deprotonation processes of the backbone amide ligands (high $pK_a$) in these cases. On the other hand, it also seems to be true that the Cu(II)-exchange rate of eq 1 is somewhat faster for proteins such as *Pf*-CopC H1F than that for peptides with similar Cu(II) binding sites such as the DP4 probe, presumably due to the Cu(II) site in the protein being preformed for binding.
(33) Martell, A. E.; Smith, R. M. *NIST Critically Selected Stability Constants of Metal Complexes Database 46, Version 8.0*; U.S. Department of Commerce, NIST Standard Reference Data Program: Gaithersburg, MD, 2004.
(34) Wernimont, A. K.; Huffman, D. L.; Finney, L. A.; Demeler, B.; O'Halloran, T. V.; Rosenzweig, A. C. *J. Biol. Inorg. Chem.* **2003**, *8*, 185−94.
(35) Arnesano, F.; Banci, L.; Bertini, I.; Thompsett, A. R. *Structure* **2002**, *10*, 1337−47.
(36) Arnesano, F.; Banci, L.; Bertini, I.; Mangani, S.; Thompsett, A. R. *Proc. Natl. Acad. Sci. U.S.A.* **2003**, *100*, 3814−9.
(37) Harford, C.; Sarkar, B. *Acc. Chem. Res.* **1997**, *30*, 123−30.
(38) Hureau, C.; Eury, H.; Guillot, R.; Bijani, C.; Sayen, S.; Solari, P.-L.; Guillon, E.; Faller, P.; Dorlet, P. *Chem.—Eur. J.* **2011**, *17*, 10151−60.
(39) Sokolowska, M.; Krezel, A.; Dyba, M.; Szewczuk, Z.; Bal, W. *Eur. J. Biochem.* **2002**, *269*, 1323−31.



DOI: 10.1021/acs.inorgchem.5b00031
*Inorg. Chem.* 2015, 54, 2950−2959